Journal of the American College of Cardiology Vol. 48, No. 1, 2006

Published by Elsevier Inc.
ISSN 0735-1097/06/$32.00
doi:10.1016/j.jacc.2006.02.054

Autonomic Innervation and Segmental Muscular Disconnections at the Human Pulmonary Vein-Atrial Junction

Implications for Catheter Ablation of Atrial-Pulmonary Vein Junction

Alex Y. Tan, MD,* Hongmei Li, MD,* Sebastian Wachsmann-Hogiu, PHD,† Lan S. Chen, MD,‡ Peng-Sheng Chen, MD, FACC,* Michael C. Fishbein, MD, FACC§

Los Angeles, California

OBJECTIVES This study sought to examine the muscle connections and autonomic nerve distributions at the human pulmonary vein (PV)-left atrium (LA) junction.

BACKGROUND One approach to catheter ablation of atrial fibrillation (AF) is to isolate PV muscle sleeves from the LA. Elimination of vagal response further improves success rates.

METHODS We performed immunohistochemical staining on 192 circumferential venoatrial segments (32 veins) harvested from 8 autopsied human hearts using antibodies to tyrosine hydroxylase (TH) and choline acetyltransferase (ChAT).

RESULTS Muscular discontinuities of widths 0.1 to 5.5 mm (1.1 ± 1.0 mm) and abrupt 90° changes in fiber orientation were found in 70 of 192 (36%) and 36 of 192 (19%) of PV-LA junctions, respectively. Although these anisotropic features were more common in the anterosuperior junction ($p < 0.01$), they were also present around the entire PV-LA junction. Autonomic nerve density was highest in the anterosuperior segments of both superior veins ($p < 0.05$ versus posteroinferior) and inferior segments of both inferior veins ($p < 0.05$ vs. superior), highest in the LA within 5 mm of the PV-LA junction ($p < 0.01$), and higher in the epicardium than endocardium ($p < 0.01$). Adrenergic and cholinergic nerves were highly co-located at tissue and cellular levels. A significant proportion (30%) of ganglion cells expressed dual adrenocholinergic phenotypes.

CONCLUSIONS Muscular discontinuities and abrupt fiber orientation changes are present in >50% of PV-LA segments, creating significant substrates for re-entry. Adrenergic and cholinergic nerves have highest densities within 5 mm of the PV-LA junction, but are highly co-located, indicating that it is impossible to selectively target either vagal or sympathetic nerves during ablation procedures. (J Am Coll Cardiol 2006;48:132–43) © 2006 by the American College of Cardiology Foundation

Radiofrequency (RF) catheter ablation in and around pulmonary veins (PVs) may cure atrial fibrillation (AF) (1). Since that original report, the techniques of AF ablation have continued to evolve. An important recent finding is that circumferential and segmental PV ablation procedures have equivalent success rates (2). This finding implies that the muscular connections around the PV- left atrium (LA) junction are naturally nonuniform, with some parts of the junction able to conduct electrical impulse better than other parts of the junction. Partial (segmental) ablation around the PV-LA junction is sufficient to interrupt electrical connections between these two structures. A second possibility is that the PV-LA junction contains certain arrhythmogenic substrates. Selective targeting of these substrates alone may contribute toward clinical success. Detailed studies of canine PV-LA junction have shown the presence of PV-LA discontinuities, especially in the anterior junction (3). These muscular discontinuities (4) and the presence of abrupt fiber orientation changes at the PV-LA junction (5) may promote PV-LA reentrant activity. However, the muscular connections at the human PV-LA junction have not been examined in detail. The first goal of this study, therefore, was to determine whether PV-LA muscular disconnections are present in human PVs, and if so, whether they are found in predictable locations such as that of canine PVs (3). A second important recent finding is that the elimination of autonomic nerves around PVs can improve the success rate of AF ablation (6). Preceding this report, others (7) have noted that reflex bradycardia and asystole may occur during RF application near the PV orifice. A bradycardic response to RF ablation was evidence of vagal nerve activation (6,7), and its subsequent disappearance with continued RF application a sign of vagal denervation (6). However, the precise anatomic localization of autonomic nerves around the orifices of human PVs remains unclear. Although cardiac nerves in the atria have been studied by many investigators (8–11), only one study (9) attempted to quantify

From the *Division of Cardiology, Department of Medicine, and the †Department of Surgery, Cedars-Sinai Medical Center, Los Angeles, California; ‡Division of Neurology, Department of Pediatrics, Los Angeles Children's Hospital and USC Keck School of Medicine, Los Angeles, California; and the §Division of Anatomic Pathology, Department of Pathology and Laboratory Medicine, David Geffen School of Medicine at UCLA, Los Angeles, California. This study was supported by a grant from the Ralph M. Parsons Foundation, Los Angeles; National Institutes of Health grants R01HL71140, R01HL78932, P01HL78931, and R01HL66389; the Cardiac Arrhythmia Research Enhancement Support Group, Inc. (CARES); the Heart Rhythm Society Fellowship in Cardiac Pacing and Electrophysiology; the Pauline and Harold Price Endowment; and the Piansky Family Trust.

Manuscript received October 6, 2005; revised manuscript received February 1, 2006, accepted February 7, 2006.

Abbreviations and Acronyms

AF = atrial fibrillation
ChAT = anticholine acetyltransferase
LA = left atrium
LIPV = left inferior pulmonary vein
LSPV = left superior pulmonary vein
PV = pulmonary vein
RF = radiofrequency
RSPV = right superior pulmonary vein
TH = antityrosine hydroxylase

the degree of innervation around the PVs specifically, but no immunostaining was performed (8,9) to distinguish between adrenergic and cholinergic nerve distributions in this region. It is therefore unclear whether RF ablation eliminates vagal (cholinergic) nerves alone or a combination of vagal and sympathetic (adrenergic) nerves. The second goal of this study, therefore, was to use immunohistochemical staining and computerized histomorphometry to determine the macroscopic and microscopic distributions of cholinergic and adrenergic nerves and ganglia around human PV orifices.

MATERIALS AND METHODS

Patient characteristics. Eight adult human hearts were obtained postmortem in 2002. None had atrial arrhythmias or a history of cardiovascular diseases or died of cardiovascular-related causes. Three patients had mild to moderate ventricular hypertrophy, but all hearts were normal histologically, with no evidence of significant coronary stenoses or myocardial pathology. Details are summarized in Table 1.

Tissue processing. Hearts were fixed 12 to 24 h after death, in 4% formalin for 1 h and then stored in 70% alcohol. Each PV was sectioned into six segments along its venous circumference. Sectioning was performed longitudinally (along the direction of blood flow). Each segment included between 7 and 20 mm of the adjoining LA. A total of 192 venoatrial segments (24 per patient) were produced. The segments were processed into paraffin blocks, and oriented to clearly visualize the epicardial and endocardial surfaces of the tissue. The paraffinized tissue blocks were cut into 5-μm-thick sections, stained as indicated, and mounted on charged slides.

Table 2. Source and Characterization of Primary Antibodies

Antigen	Antibody Vendor	Antibody Dilution
Tyrosine hydroxylase	Accurate; Westbury, NY	1:100
Choline acetyltransferase	Chemicon; Temecula, CA	1:50–1:100
GAP 43	Chemicon; Temecula, CA	1:100
Neurofilament	Dako; Carpinteria, CA	1:300
Synaptophysin	Dako; Carpinteria, CA	1:100

GAP 43 = growth-associated protein 43.

Histochemistry and immunohistochemistry. For each paraffin block, one slide each was stained with hematoxylin and eosin and Mason trichrome to accentuate muscle and connective tissues. Serial sections were used for immunostaining by the avidin-biotin complex method as described previously (12). Antityrosine hydroxylase (TH) antibodies were used to label adrenergic nerves, and anticholine acetyltransferase (ChAT) antibodies were used to label cholinergic nerves. Table 2 illustrates all antibodies used.

Nerve density determination. Nerve density was quantified by a single blinded investigator, using computer-assisted histomorphometry (ImagePro, Media Cybernetics, Silver Spring, Maryland) (12). We analyzed nerve densities in multiple target regions to determine autonomic nerve distributions along the longitudinal and transmural axes of every venoatrial segment, and circumferentially, across the six segments per vein.

Fluorescent double staining and confocal microscopy. Fluorescent dual-labeling with TH and ChAT was performed to determine whether there was colocalization of adrenergic and cholinergic nerves within nerve trunks/ganglia. Dual-labeled sections were visualized with a laser-scanning confocal microscope, with digital manipulations restricted to conventional photographic techniques only.

Analysis of structural anisotropy. We examined the patterns of muscular connections between PV and LA at the venoatrial junction under light microscopy using slides stained with hematoxylin and eosin and Mason trichrome stains. All 192 sections from 32 veins were systematically

Table 1. Clinical Characteristics

Patient No.	Age	Gender	Ethnicity	Cause of Death	Body Weight (kg)	Height (cm)	Heart Weight (g)	Cardiac Findings Postmortem
1	37	F	Caucasian	Spinocerebellar ataxia type III	43	154	200	UR
2	72	F	African American	Cerebral lymphoma	68	175	NA	UR
3	63	F	African American	End-stage liver disease	98	155	NA	UR
4	31	F	Caucasian	Large-cell lymphoma	45	160	350	Hypertrophy
5	54	F	Caucasian	Acute fulminating hepatitis, unknown etiology	130	177	600	Hypertrophy
6	67	M	Caucasian	Disseminated esophageal adenocarcinoma	82	174	375	UR
7	72	F	Caucasian	Systemic candidiasis after multiabdominal organ transplantation	59	175	400	Hypertrophy
8	65	F	Caucasian	Septic shock	70	165	325	UR

NA = not available; UR = unremarkable.

examined for: 1) disconnections between PV and LA muscle sleeves, 2) abrupt and extreme (90°) changes in fiber orientation, and 3) reductions in muscle sleeve thickness from LA to PV. The circumferential distributions of these parameters were then mapped. The PV muscle sleeve thickness was measured perpendicular to the direction of blood flow, at two locations, 2 mm away from each other at the PV-LA junction. The difference between the two was expressed as a percentage of the greater value.

Statistical analysis. Quantitative data were presented as mean ± standard deviation. Paired student *t* test was used to compare the means between two groups, whereas analysis of variance with Newman-Keuls post hoc analyses was used for differences between multiple groups. Where appropriate, chi-square test was used. A p value <0.05 was considered significant.

RESULTS

Gross anatomy. A total of 192 venoatrial segments were obtained from 32 veins in 8 patients. Among them, 51 of 192 segments had no PV muscle sleeve or had small islands of muscle only, whereas the remainder (n = 141) had a 15.1 ± 5.9 mm length of PV muscle sleeve. Each segment included 12.3 ± 3.9 mm of adjoining LA muscle (range 7 to 20 mm).

Muscle connections and fiber orientation at PV-LA junctions. The myofascial architecture at the venoatrial junction was highly complex, with segmental disconnections, fiber orientation changes, and changes in muscle sleeve thickness. Grossly, three patterns (Fig. 1A) of PV-LA muscular connections were observed. In Pattern 1, PV and LA muscle sleeves were disconnected. In Patterns 2 and 3, there was uninterrupted connection between PV and LA muscle. This connection was complex in Pattern 2 because of multiple muscle sleeves oriented at different angles but smooth in Pattern 3 because of relatively uniform myocyte orientation at the junction. Every vein had at least one segment that had no muscle or Pattern 1. In 26 of 32 veins, there was at least one segment with uninterrupted connection between PV and LA muscle (Pattern 2 or 3). In the remaining six veins (right superior pulmonary vein

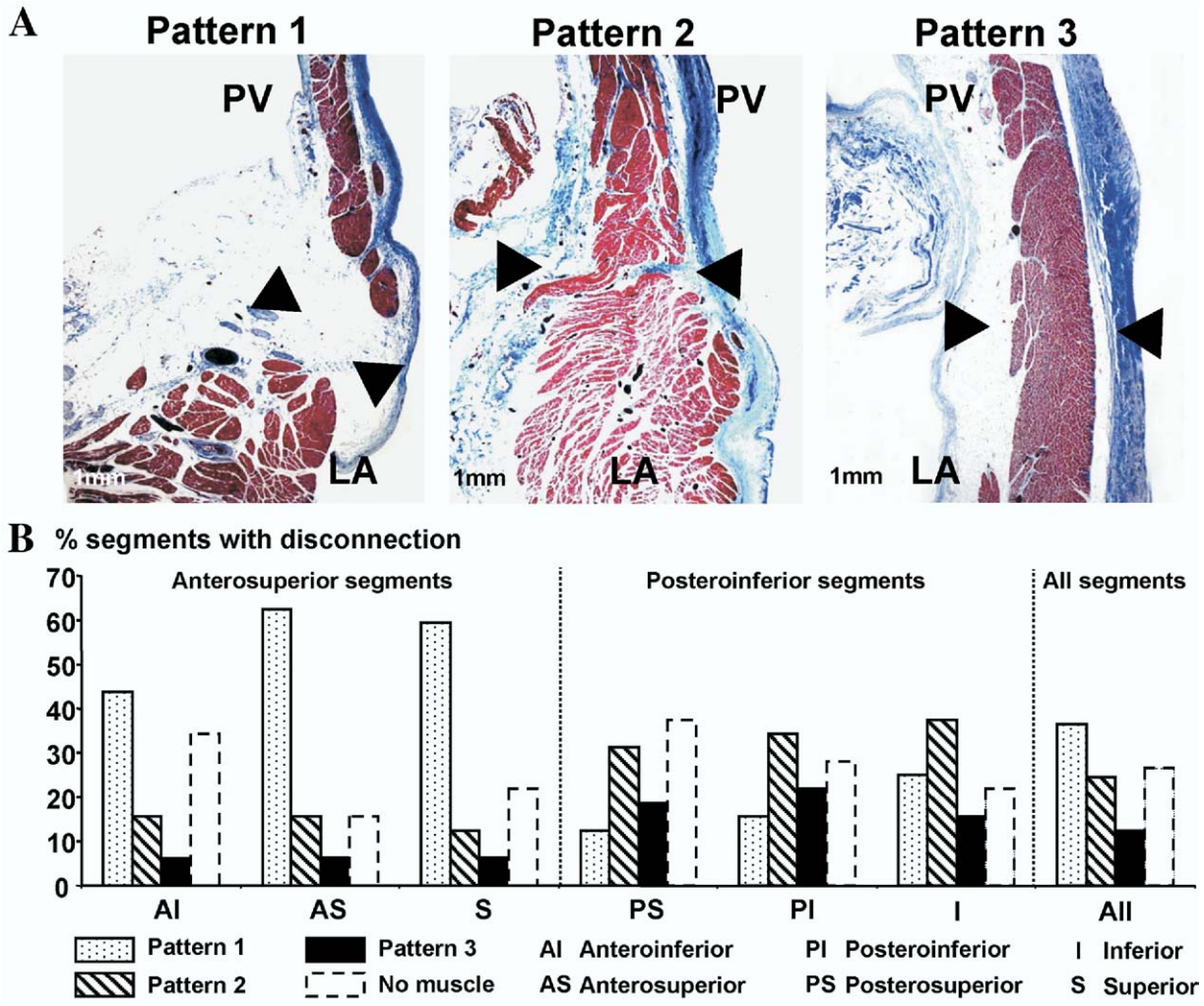

Figure 1. Patterns of pulmonary vein (PV)-left atrium (LA) connections. **(A)** Three patterns of PV-LA connections, from disconnected (Pattern 1) to well connected (Pattern 3). **(B)** Circumferential distributions.

[RSPV] 3, left superior pulmonary vein [LSPV] 2, left inferior pulmonary vein [LIPV] 1), there was no connection between PV and LA muscle at all (either Pattern 1 or no muscle). Figure 1B summarizes the circumferential distribution of these patterns. In the anterosuperior segments, the most common pattern observed was Pattern 1. In the posteroinferior segments, there was no one dominant pattern. Overall, 70 segments (36%) had Pattern 1, 47 (24%) had Pattern 2, 24 (13%) had Pattern 3 and 51 (27%) had no muscle.

Figures 2A1 to 2A3 show further quantitative analyses of PV-LA muscular disconnections. Figure 2A1 illustrates the PV-LA muscular gap. In these 70 segments, the mean gap between PV and LA myocardium was 1.1 ± 1.0 mm (range 0.1 to 5.5 mm) (Fig. 2A2). A majority (n = 53 of 70, 76%) of segments with PV-LA disconnection were located in the anterosuperior as opposed to the posteroinferior (n = 17 of 70, 24%, $p < 0.001$) junction (Fig. 2A3). However, disconnections were also found in other areas around the PV orifice (Fig. 1B). Figures 2B1 and 2B2 are two examples of abrupt reductions in muscle sleeve thickness at the PV-LA junction. Figure 2C1 highlights the presence of abrupt 90° changes in myocyte orientation at the PV-LA junction. Figure 2C2 is a high-power view of the area enclosed by the square in Figure 2C1, the arrow showing the direction of fiber orientation change. The degree of muscle sleeve thinning was greater at anterosuperior than posteroinferior junctions ($p = 0.01$) (Fig. 2C3). There were 46 of 192 PV-LA junctions where abrupt 90° changes in fiber orientation were found. Among them, 34 were in the anterior junction and 12 were in the posterior junction ($p < 0.001$). For every one of the 192 segments, serial sectioning showed consistency of each of the abovementioned features over a 0.2-mm thickness. In 20 of 192 randomly selected segments, serial sectioning up to 2-mm thickness showed that muscular disconnections persisted through that length along the venous circumference.

Distributions of adrenergic and cholinergic nerves. Figure 3 shows examples of nerves and ganglia immunoreactive to markers specific for nerves. Among them, GAP 43 is a marker

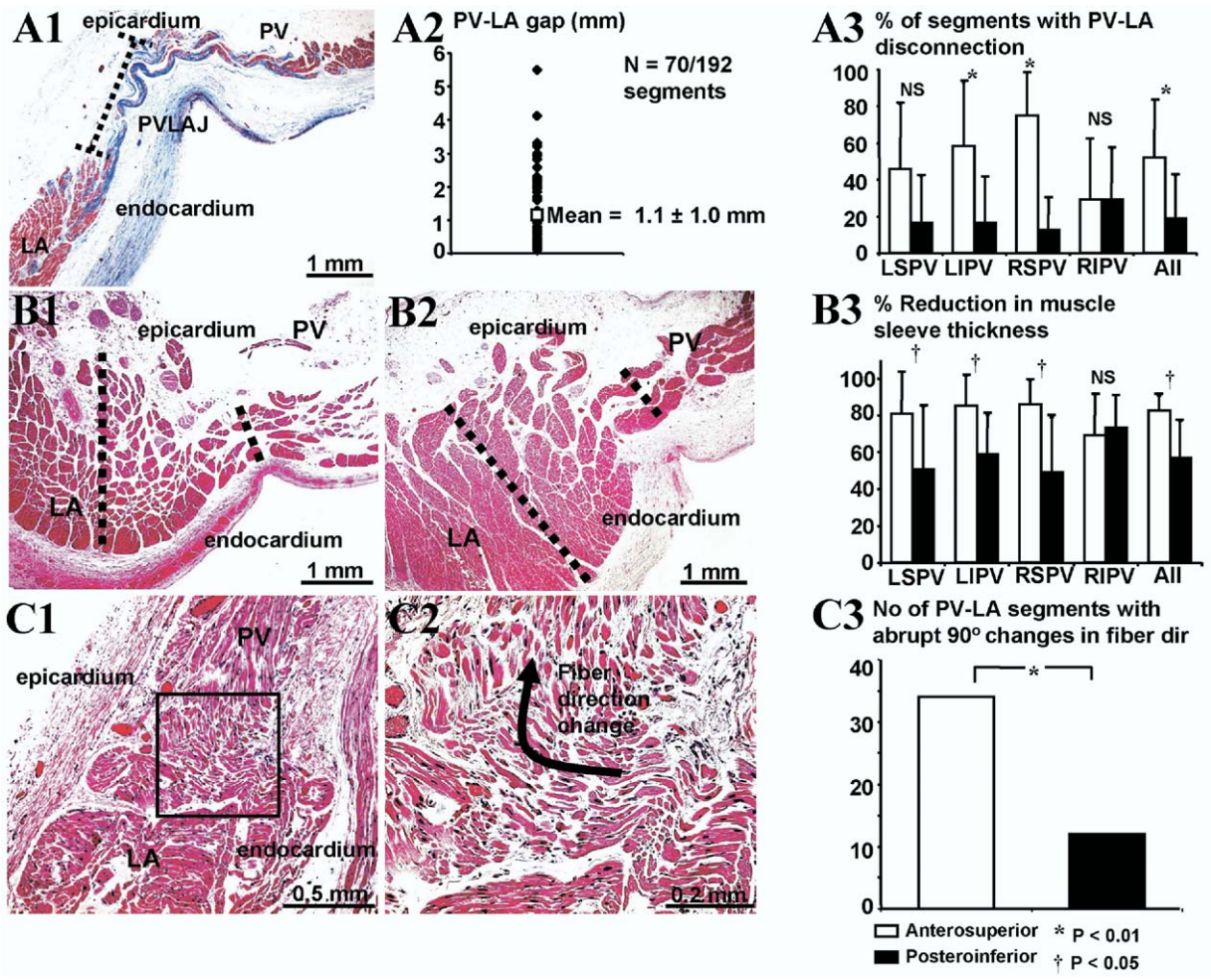

Figure 2. Circumferential distributions of muscular discontinuities and fiber orientations at the pulmonary vein (PV)-left atrium (LA) junction. **(A1)** The PV-LA gap (dotted line segment). **(A2)** Mean length of the PV-LA gap. **(A3)** Circumferential distribution of disconnected segments. **(B1, B2)** Two examples of abrupt reduction in muscle sleeve thickness at the PV-LA junction. **(B3)** The extent of reductions in muscle sleeve thickness at the anterosuperior versus posteroinferior junctions. **(C1)** Abrupt 90° changes in fiber direction at the PV-LA junction. **(C2)** High-power view of the boxed area in **C1**. **(C3)** Distribution of segments with this pattern. LIPV = left inferior pulmonary vein; LSPV = left superior pulmonary vein; RIPV = right inferior pulmonary vein; RSPV = right superior pulmonary vein.

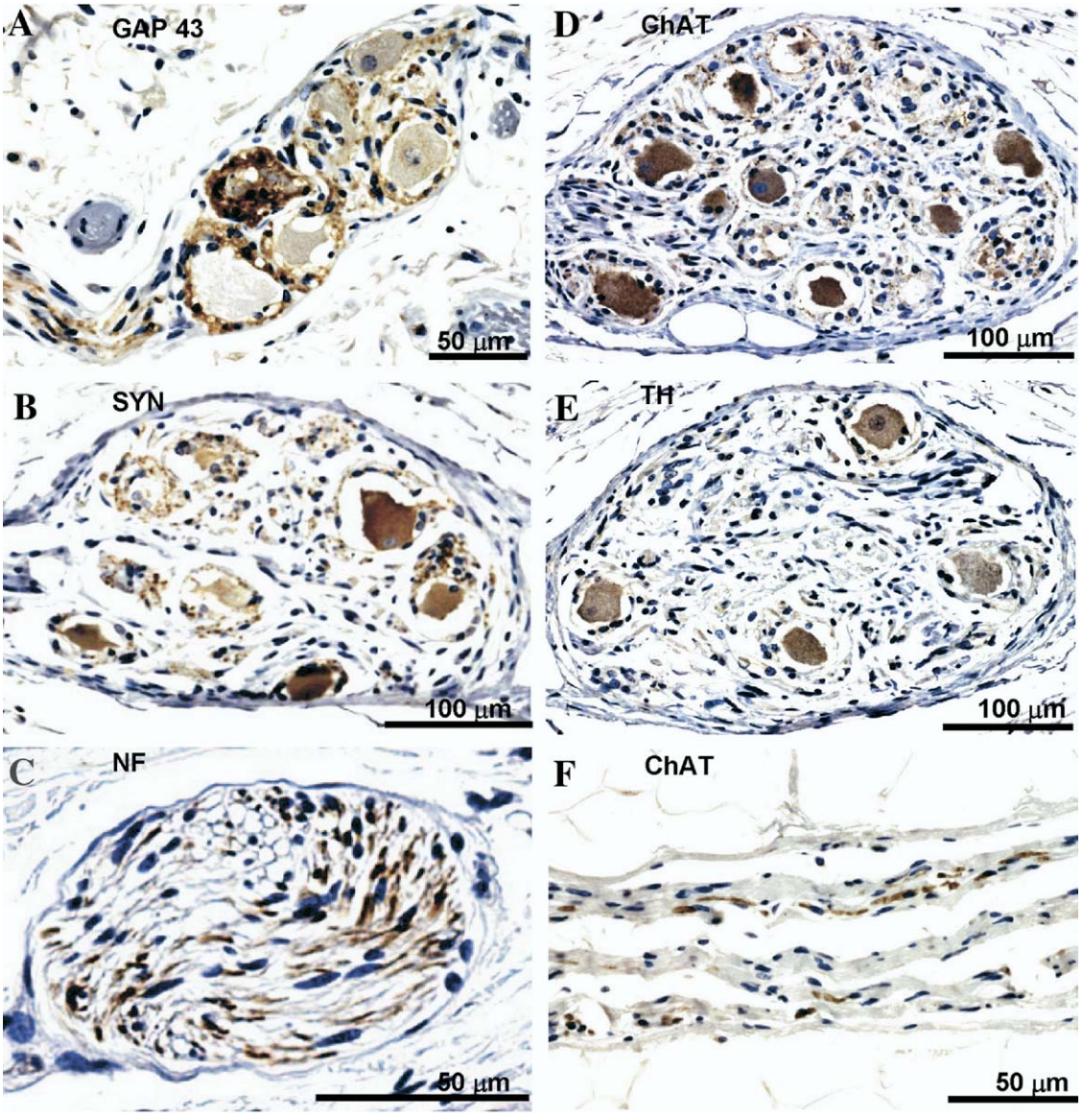

Figure 3. Examples of immunohistochemical staining results in cardiac ganglia and nerves. **(A)** Growth-associated protein 43 (GAP 43) demonstrating axonal growth within the ganglion; **(B)** synaptophysin (SYN) staining demonstrating synaptic endings; **(C)** neurofilament (NF) staining confirming the presence of nerve fibers; **(D)** choline acetyltransferase (ChAT) staining showing cholinergic nature of most ganglion cells; **(E)** tyrosine hydroxylase (TH) staining showing co-localization of adrenergic cells within the same ganglion; and **(F)** ChAT positivity of nerve adjacent to ganglion.

of axonal growth, neurofilament is expressed by axonal and dendritic processes and synaptophysin expressed at synaptic endings (12). Positive stains of these neurospecific antigens confirmed that these structures were cardiac nerves. We observed thin nerve fibrils (diameters <20 μm), large nerve fiber trunks (≤ 600 μm in diameter) and cardiac ganglia (≤ 500 μm in diameter, containing 1 to 12 neuronal cell bodies).

LONGITUDINAL AND TRANSMURAL NERVE DISTRIBUTIONS. Figure 4A illustrates the longitudinal distribution of autonomic nerves from LA to distal PV. Although adrenergic nerve densities were several-fold that of cholinergic nerve densities, both nerve densities were highest in the LA region within 5 mm from the PV-LA junction, as opposed to further (>5 mm) away from the junction ($p < 0.01$) or in the PV ($p < 0.01$). Transmurally (Fig. 4B), epicardial nerve trunks and ganglia were larger and more numerous than those in the endocardium, accounting for markedly greater nerve density in the epicardial half of tissue.

CIRCUMFERENTIAL DISTRIBUTION. We analyzed nerve densities between the following pooled averages: anterior (average of anterosuperior and anteroinferior) versus posterior (average of posterosuperior and posteroinferior) segments, and superior (average of superior, anterosuperior, and posterosuperior) versus inferior (average of inferior, anteroinferior, and posteroinferior) segments. For both nerve types, nerve density was greater in the superior > inferior aspects of the LSPV ($p < 0.05$); inferior > superior aspects of the LIPV ($p < 0.05$); anterosuperior > posteroinferior aspects

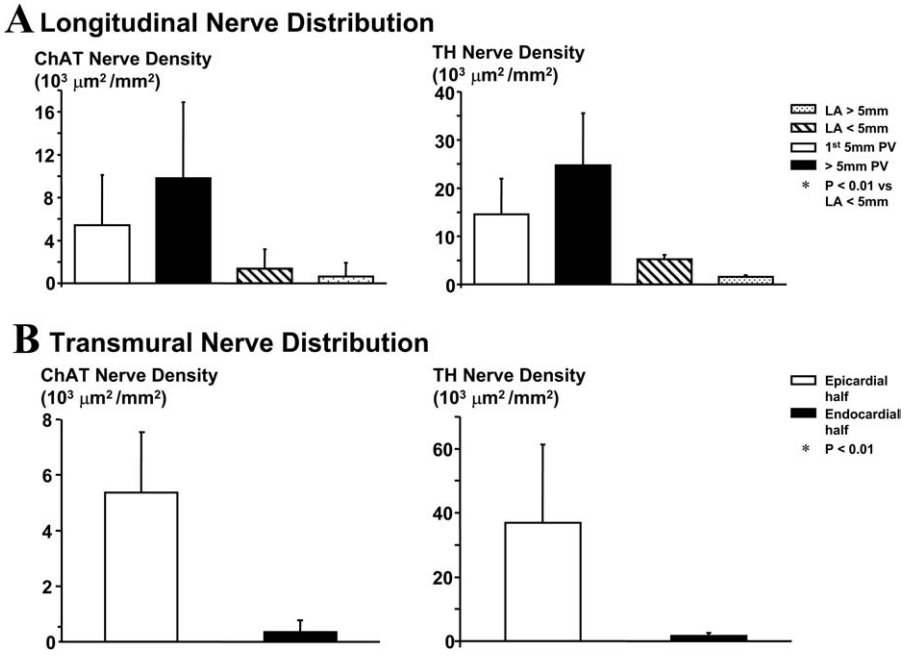

Figure 4. Longitudinal **(A)** and transmural **(B)** autonomic nerve distribution. ChAT = anticholine acetyltransferase; LA = left atrium; TH = antityrosine hydroxylase.

of the RSPV ($p < 0.05$); and posteroinferior > anterosuperior aspects of the RIPV ($p < 0.05$). These results are summarized in Table 3 and diagrammatically in Figure 5.

Taken together, the data in Figures 4 and 5 show that adrenergic and cholinergic nerves have spatially similar distributions along the longitudinal and transmural axes of PV-LA segments and circumferentially around each PV orifice.

Functional differentiation of adrenergic and cholinergic nerves. CO-LOCATION OF ADRENERGIC AND CHOLINERGIC NERVES AT TISSUE AND CELLULAR LEVELS. At a tissue level, there were no discrete regions of adrenergic or cholinergic nerve predominance. Instead both nerve types clustered together to form a single neural plexus (Figs. 6A1 to 6A5). Figure 6A5 is a composite image of a dual TH- and ChAT-labeled section through the LIPV-LA junction, showing the co-location of cholinergic ganglia (arrowheads) and adrenergic nerve trunks (arrows) within the plexus.

At a cellular level, adrenergic and cholinergic nerves were present within the same nerve fiber trunk (Figs. 6B1 to 6B2 and 6D1 to 6D3) or cardiac ganglia (Figs. 6C1 to 6C2 and 6E1 to 6E3). Approximately 60% of nerve fiber trunks were purely adrenergic, 10% were purely cholinergic, and 25% were mixed, i.e., contained mixtures of adrenergic and cholinergic nerves within the same neural envelope. A minority (5%) were immunoreactive to neither TH nor ChAT. The vast majority (>95%) of ganglion cells were cholinergic. However, over 90% of ganglia also contained adrenergic nerve fibers. For example, in Figures 6C1 to 6C2, the same ganglion contained a cholinergic ganglion cell (arrow, Fig. 6C1) and adrenergic nerve fibers (arrow, Fig. 6C2).

ADRENOCHOLINERGIC NEURAL CONNECTIONS WITHIN GANGLIA. Figure 7A1 is a low-power view of a ganglion containing both TH and ChAT immunopositive ganglion

Table 3. Circumferential Nerve Densities at the PV-LA Junction

Nerve Type	Anterior vs. Posterior Segments			Superior vs. Inferior Segments		
	Anterior	Posterior	p	Superior	Inferior	p
TH nerve density (10^3 $\mu m^2/mm^2$)						
LSPV	21.04 ± 39.73	17.05 ± 32.38	0.42	22.57 ± 27.08	9.41 ± 16.80	0.03
LIPV	13.12 ± 14.17	9.12 ± 6.71	0.20	4.91 ± 3.88	23.50 ± 24.86	0.02
RSPV	31.45 ± 36.20	11.00 ± 17.19	0.03	24.65 ± 26.74	12.78 ± 20.31	0.05
RIPV	11.49 ± 9.41	4.85 ± 5.52	0.03	4.82 ± 5.43	13.04 ± 9.96	0.009
ChAT nerve density (10^3 $\mu m^2/mm^2$)						
LSPV	0.85 ± 0.52	1.41 ± 1.77	0.24	2.85 ± 1.77	0.25 ± 0.28	0.003
LIPV	1.21 ± 1.69	2.58 ± 1.54	0.05	0.27 ± 0.27	3.68 ± 1.98	0.003
RSPV	2.43 ± 1.07	0.58 ± 0.59	0.003	1.98 ± 0.90	0.50 ± 0.51	0.009
RIPV	0.34 ± 0.21	3.59 ± 2.47	0.01	0.21 ± 0.29	2.47 ± 2.00	0.008

ChAT = anticholine acetyltransferase; LA = left atrium; LIPV = left inferior pulmonary vein; LSPV = left superior pulmonary vein; PV = pulmonary vein; RIPV = right inferior pulmonary vein; RSPV = right superior pulmonary vein; TH = antityrosine hydroxylase.

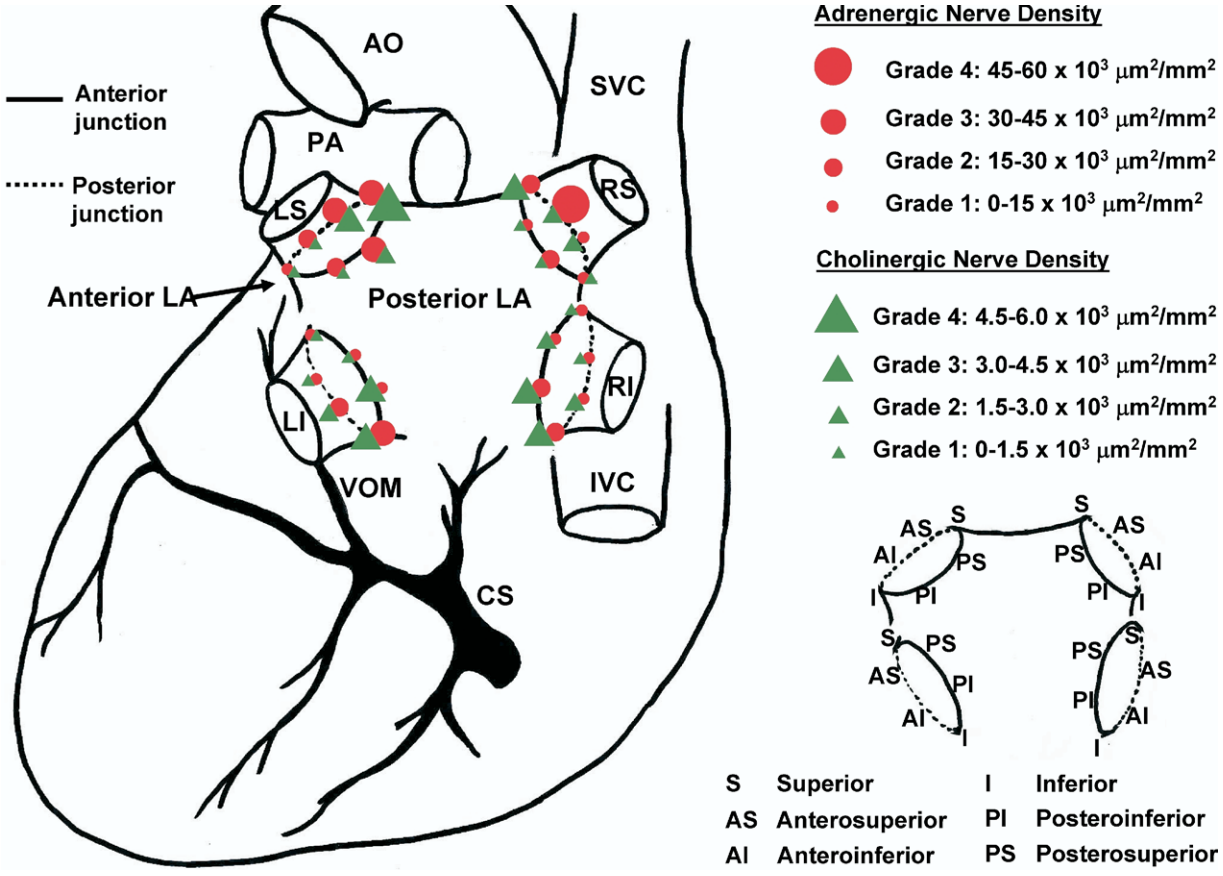

Figure 5. Circumferential distribution of autonomic nerves at the pulmonary vein (PV)-left atrium (LA) junction. AO = aorta; CS = coronary sinus; IVC = inferior vena cava; LA = left atrium; LI = left inferior pulmonary vein; LS = left superior pulmonary vein; PA = pulmonary artery; PV = pulmonary veins; RI = right inferior pulmonary vein; RS = right superior pulmonary vein; SVC = superior vena cava; VOM = vein of marshall.

cells and nerve fibers. Figures 7A2 to 7A4 are higher-power views. Figure 7A2 shows a ChAT-positive cell body (C). In Figure 7A3, speckled TH staining (arrow) was observed at the lower edge of this cell (C). The composite image in Figure 7A4 shows that TH and ChAT colocalization (yellowish stain) was not present in the neuroplasm, but was limited to the lower edge (arrow) of the cell body (C). The granular nature of colocalized staining suggests adrenergic neural processes (P) establishing axosomatic synapses with cholinergic cell bodies (C) within the ganglia.

BIPHENOTYPIC ADRENOCHOLINERGIC GANGLION CELLS. In the previous examples, TH and ChAT immunopositivity were present within the same structure but not the same cell. However, 30% of ganglion cells showed simultaneous TH and ChAT immunopositivity within the neuroplasm. Figure 7B1 is a low-power view of a ganglia double-stained with TH and ChAT. Figures 7B2 to 7B4 are high-power views of its contents. In Figure 7B2, the cell body in the center of the ganglia (arrowhead) was ChAT-positive. Within the same cell, TH immunopositivity was present and consisted of brightly fluorescent specks on a background of more diffuse staining (Fig. 7B3, arrowhead), suggesting immunoreactivity not only of neural processes (specks) but also of the neuroplasm proper (diffuse staining). The co-localization of ChAT and TH within the neuroplasm proper (diffuse yellowish stain of cell in Fig. 7B4) suggests that ganglion cells can potentially express both cholinergic and adrenergic markers simultaneously, possibly in the process of a neurochemical switch in response to external stimuli (13).

Effect of left ventricular hypertrophy and age. Left ventricular hypertrophy and age did not significantly affect the presence of muscular discontinuities, abrupt 90° fiber orientation changes, muscle sleeve thinning, or autonomic nerve densities in this cohort (Table 4).

DISCUSSION

We performed immunostaining to distinguish between adrenergic and cholinergic nerves at the human PV-LA junction, and examined in detail the patterns of muscular connections between PV and LA. We have shown that: 1) PV-LA muscular discontinuities and abrupt 90° changes in myofiber orientation were present in the PV-LA junction in over half of all segments examined; 2) although these anisotropic features were found more frequently in the anterosuperior than posteroinferior junctions, they seem to have a more widespread distribution than that of canine PVs (3); 3) adrenergic and cholinergic nerve densities were

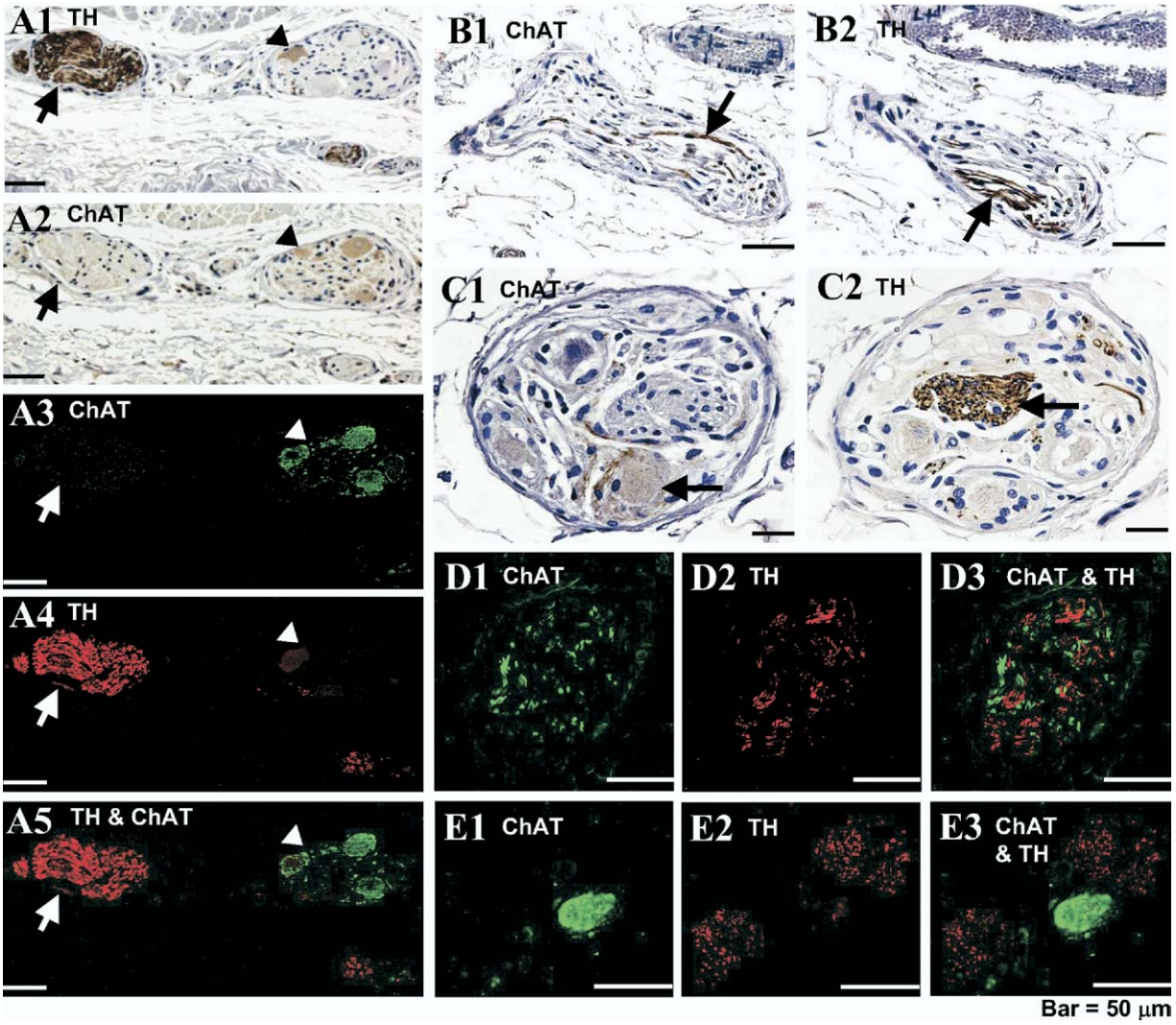

Figure 6. Co-location of adrenergic and cholinergic nerves at a tissue level **(A1 to A5)** and at a cellular level within nerve fiber trunks **(B1 to B2, D1 to D3)** and cardiac ganglia **(C1 to C2, E1 to E3)**. See text for explanations. ChAT = anticholine acetyltransferase; TH = antityrosine hydroxylase.

highest in the LA within 5 mm from the PV-LA junction, higher in the superior aspect of LSPV, anterosuperior aspect of RSPV, and inferior aspects of the both inferior PVs than diametrically opposite, and higher in the epicardial than endocardial half of the tissue; and 4) adrenergic and cholinergic nerves were highly co-located at tissue and cellular levels of spatial organization. Interestingly, a significant (30%) proportion of ganglion cells expressed both adrenergic and cholinergic markers simultaneously. These findings suggest that: 1) the PV-LA junction contains anatomical substrates (muscular discontinuities and abrupt fiber orientation changes) to support re-entry; 2) there are no good empiric targets for segmental PV isolation because of the widespread distributions of PV-LA muscular discontinuities; 3) the LA region close to the PV-LA junction rather than farther away in the LA or PV would be the most appropriate target for autonomic modulation procedures; and 4) it is not possible to selectively ablate either adrenergic or cholinergic nerves in this location because both nerve types are highly co-located in this region.

PV-LA muscular disconnection. There are two major clinical implications of muscular discontinuity at the PV-LA junction. In animal models of experimental AF, the junction is frequently a preferential site of focal discharge and re-entry that serves as a high-frequency source during AF (5,14,15). Because tissue anisotropy may contribute to these observations, the anatomy of human PVs has been intensely examined (16,17). However, these studies did not focus on the structure of the PV-LA junction proper. Spach et al. (4) showed that muscular discontinuities of >1 mm may cause unidirectional block. In this study, we found gaps between PV and LA muscle with an average length of just over 1 mm. Admittedly, longer gaps such as 5.5 mm may halt impulse propagation bidirectionally. However, such large gaps are uncommon (78% of segments had gaps of 2 mm or less, 96% had gaps of 3 mm or less). Shorter gaps

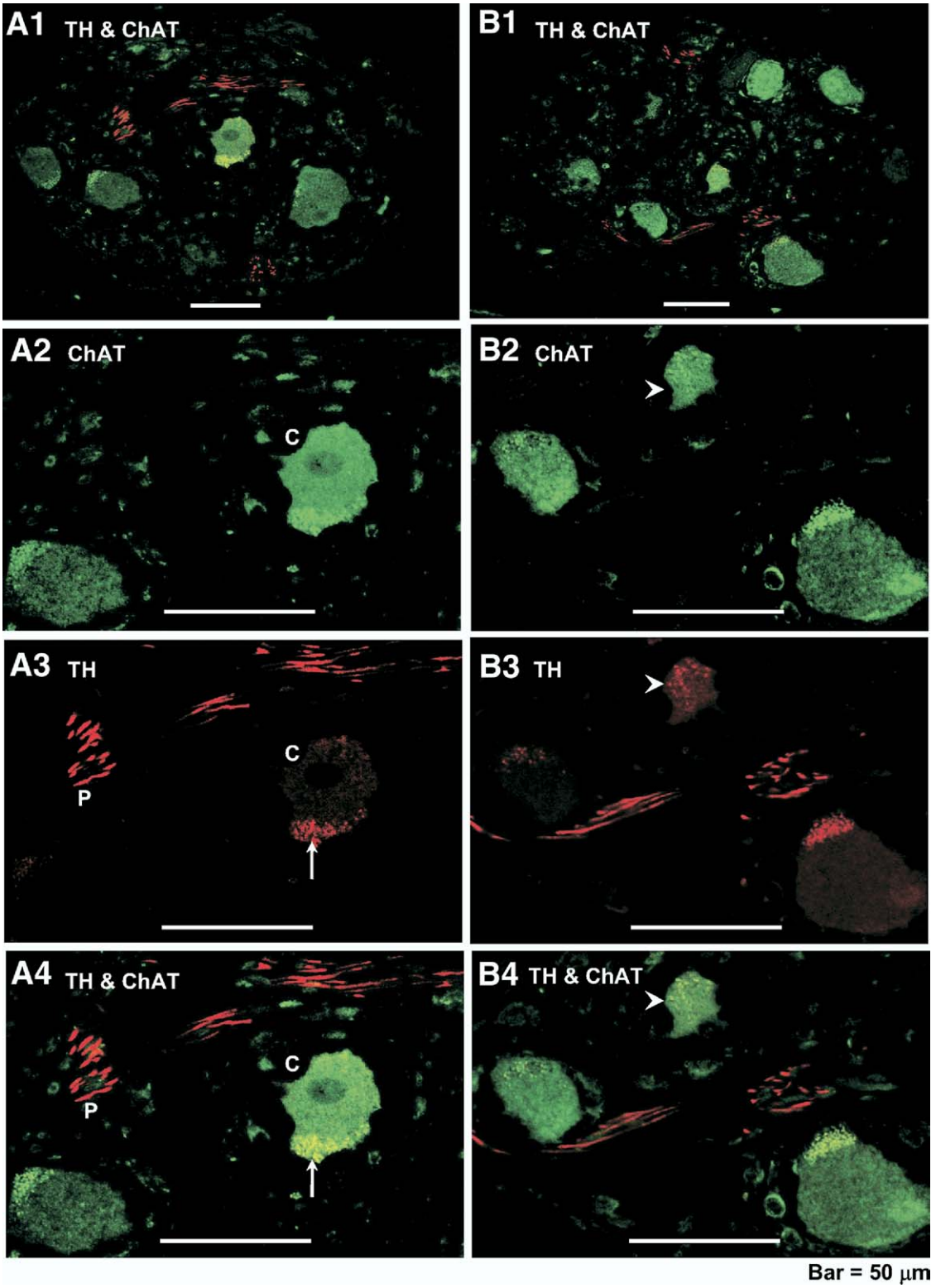

Figure 7. Adrenocholinergic neural connections within cardiac ganglia **(A1 to A4)**, and ganglion cells expressing dual adrenergic and cholinergic phenotypes **(B1 to B4)**. ChAT = anticholine acetyltransferase; TH = antityrosine hydroxylase.

may reduce the safety factor of propagation sufficiently to cause unidirectional block, but favorable source-sink conditions may allow propagation in the opposite direction to create anisotropic re-entry. In addition, abrupt changes in fiber orientation and muscle sleeve thickness at the junction may promote re-entry (18) even without actual muscular discontinuities, by slowing propagation and allowing sufficient time for refractory tissue to recover.

Table 4. Effect of Age and Left Ventricular Hypertrophy on Structural Features and Autonomic Nerve Density

Main Findings	Age (r^2)*	LVH		
		LVH (n = 3)	Non-LVH (n = 5)	p
PV-LA muscular disconnection (% of segments)	−0.25	36.1 ± 8.6	37.5 ± 15.6	0.63
90° fiber orientation changes (% of segments)	0.0047	23.3 ± 16.6	16.9 ± 3.5	0.34
Abrupt muscle thinning (%)	0.0019	69.5 ± 6.7	70.0 ± 10.4	0.47
Mean adrenergic nerve density per vein (10^3 $\mu m^2/mm^2$)	0.084	10.73 ± 12.80	13.87 ± 9.15	0.44
Mean cholinergic nerve density per vein (10^3 $\mu m^2/mm^2$)	0.0042	1.02 ± 0.27	1.58 ± 0.74	0.13

*r^2 = correlation coefficient.
LVH = left ventricular hypertrophy; other abbreviations as in Table 1.

The segmental ablation approach attempts to target only those segments with good PV-LA connections to achieve electrical disconnection and minimize the risks of PV stenosis. However, we could not identify any empiric targets for segmental ablation because PV-LA muscular disconnections were not exclusive to any particular segment. Nevertheless, because PV-LA junctions are naturally disconnected partly around each vein, it is not necessary to perform RF ablation all around the PV to achieve successful PV isolation or to significantly reduce electrical connections between PV and LA. Our findings may, in part, explain the results of a recent report (2) showing that segmental ostial ablation is as effective as circumferential LA ablations in the treatment of AF.

Quantitative distribution of adrenergic and cholinergic nerves. Quantitative and qualitative anatomic studies on human cardiac autonomic nerves have previously been undertaken (8,10,11). However, only one study (9) attempted to quantify nerves within PVs specifically, although not to the detail currently provided. Our study extended their observations by using immunostaining to distinguish between adrenergic and cholinergic nerves, and by using histomorphometric methods to quantify nerve density. We used ChAT immunostaining to identify cholinergic nerves, instead of traditional histochemical methods that detect acetylcholinesterase, because the specificity of the latter technique is limited because of the expression of acetylcholinesterase by noncholinergic neurons (19).

We found up to a five-fold magnitude difference in innervation density between the patient with the lowest innervation density and that with the highest. This was most likely attributable to intrinsic differences in innervation rather than being technique-related, because the segments with little staining were generally devoid of nerves. Finally, cardiac nerve staining in autopsied hearts has historically been a challenge because of fixation lag time. In this study, however, all hearts were fixed within a time frame on par with that reported previously (10). Because strong staining was observed in all cases, it is unlikely that the differences in nerve density were caused by autolysis.

Comparison with previous clinical and experimental data. Recent clinical reports indicate that the bradycardic response can be most frequently elicited by stimulating or ablating in certain regions around the PV-LA junction (6,20). These include the roof junction of the left superior PV, posteroinferior junctions of both inferior veins, and anterior junction of the right superior PV. The investigators postulated that these regions contained higher degrees of innervation than other parts of the atria. The current anatomical study supports this hypothesis and identifies the anterosuperior aspects of the superior PVs and inferior aspects of the inferior PVs as sites with highest nerve densities. These localizations also parallel four of the five atrial ganglionated plexuses defined by Armour et al. (8) using gross anatomical analyses of whole-mounted human hearts. A novel aspect of the present study is the demonstration of adrenocholinergic neural intermixtures within these plexuses. We also found that nerve densities within the PV were markedly lower than that outside the PV, and may partly explain the lower incidence of bradycardic response when ablating within PVs (7,21) compared with outside the PVs (6,20).

Some differences exist between the present anatomical study and clinical reports. Contrary to the notion that bradycardia represents vagal (cholinergic) nerve activation (6,7), the present study indicates that it would be impossible to separately activate either cholinergic or adrenergic nerves because of their close positions and interconnections. By the same token, the disappearance of bradycardia does not imply vagal denervation alone. If both nerves are activated at the same time, why is bradycardia observed and not tachycardia? Tsai et al. (7) hypothesized that bradycardia was caused by activation of the Bezold Jarisch reflex, which is mediated through the vagi and cranial medullary centers that control heart rate, vasomotor tone, and respiration (22). Functional efferent vagal pathways then converge on the aortic root fat pad, before projecting to sinus and AV nodes (23). Microinjection of retrograde neural tracer into the sinus node resulted in the appearance of the tracer within these perivenous plexuses, chiefly around the right PV (24). These studies suggest that complex neural pathways are involved in the generation of the bradycardic response. The noninvolvement of sympathetic nerves in this pathway may explain the absence of tachycardia. The local release of acetylcholine from predominantly cholinergic ganglion cells may be an additional paracrine mechanism contributing to

bradycardic prominence. Furthermore, we found that a higher proportion of ganglion cells in the PV region were cholinergic (>95%) compared with 80% in adult human nodal tissue (11). A common observation after AF ablation is a reduction in heart rate variability, suggesting sympathetic overbalance. Therefore, a third possible mechanism of bradycardia is the disruption of sympathovagal balance in favor of sympathetic activation. In support of this hypothesis, both we and Marron et al. (10) found that adrenergic nerves were more widely distributed than cholinergic nerves, implying that PV ablation eliminates a greater proportion of total atrial parasympathetic than sympathetic innervation. Further studies are required to elucidate the relative contributions of these mechanisms. For example, it would be helpful to investigate the adrenergic versus cholinergic preponderance of efferent projections from PVs to nodal tissue. However, this would require the use of whole-mounted hearts and is therefore beyond the scope of the present study.

In summary, the evidence to date supports the hypothesis that autonomic nerve response during stimulation/ablation procedures is dependent on local nerve distribution. However, the induction of bradycardia does not imply activation of vagal nerves alone.

Biphenotypic ganglion cells. An interesting finding of this study is the presence of ganglion cells that expressed both adrenergic and cholinergic phenotypes, a phenomenon that could be explained by the work of Schafer et al. (13). They reported that fully functional adrenergic neurons arising from principal ganglion cells, which initially lack cholinergic expression, may undergo a switch from adrenergic to cholinergic phenotype under the influence of factors secreted by effector sites, such as the sweat gland. This induces attenuation of adrenergic expression and development of cholinergic expression. The data highlight the possibility that human adult ganglion cells in and around PVs may undergo neurochemical remodeling in response to external stimuli, such as structural heart disease.

Study limitations. Although the number of patients was relatively small, staining for both TH and ChAT was performed for all 192 venoatrial segments unselectively and without exception. This study, therefore, provides a detailed circumferential distribution of PV-LA muscle connections and autonomic nerves in that region. Because most patients were female, no conclusions regarding gender differences could be made. Finally, this is a purely anatomical study without electrophysiological measurements from the same patients. The physiological relevance of the spatial colocalization of adrenergic and cholinergic nerves could only be inferred based on published reports (6,20).

Conclusions. We have shown that the anatomical milieu of the human PV-LA junction is intrinsically favorable to the formation of re-entrant activations. Secondly, we have provided detailed anatomical maps of both adrenergic and cholinergic innervation of the PV-LA junction. Our findings indicate that both nerve types are most densely located in the LA closer to the junction than further away in the LA or PV, but because they are highly co-located in this region, the findings imply that it is impossible to selectively eliminate either nerve type during ablation procedures. Finally, we have shown that a significant proportion of cardiac neuronal cells expressed both adrenergic and cholinergic phenotypes simultaneously, suggesting a capacity for neurochemical plasticity.

Acknowledgment

The authors thank Dr. C. Thomas Peter for his support.

Reprint requests and correspondence: Dr. Michael C. Fishbein, Department of Pathology and Laboratory Medicine, UCLA School of Medicine, Room 13-145H, 10833 Le Conte Avenue, Los Angeles, California 90095-1732. E-mail: mfishbein@mednet.ucla.edu.

REFERENCES

1. Haissaguerre M, Jais P, Shah DC, et al. Spontaneous initiation of atrial fibrillation by ectopic beats originating in the pulmonary veins. N Engl J Med 1998;339:659–66.
2. Karch MR, Zrenner B, Deisenhofer I, et al. Freedom from atrial tachyarrhythmias after catheter ablation of atrial fibrillation: a randomized comparison between two current ablation strategies. Circulation 2005;111:2875–80.
3. Hamabe A, Okuyama Y, Miyauchi Y, et al. Correlation between anatomy and electrical activation in canine pulmonary veins. Circulation 2003;107:1550–5.
4. Spach MS, Miller WT Jr., Dolber PC, Kootsey JM, Sommer JR, Mosher CE. The functional role of structural complexities in the propagation of depolarization in the atrium of the dog. Cardiac conduction disturbances due to discontinuities of effective axial resistivity. Circ Res 1982;50:175–91.
5. Chou CC, Nihei M, Zhou S, et al. Intracellular calcium dynamics and anisotropic re-entry in isolated canine pulmonary veins and left atrium. Circulation 2005;111:2889–297.
6. Pappone C, Santinelli V, Manguso F, et al. Pulmonary vein denervation enhances long-term benefit after circumferential ablation for paroxysmal atrial fibrillation. Circulation 2004;109:327–34.
7. Tsai CF, Chen SA, Tai CT, et al. Bezold-Jarisch-like reflex during radiofrequency ablation of the pulmonary vein tissues in patients with paroxysmal focal atrial fibrillation. J Cardiovasc Electrophysiol 1999;10:27–35.
8. Armour JA, Murphy DA, Yuan BX, Macdonald S, Hopkins DA. Gross and microscopic anatomy of the human intrinsic cardiac nervous system. Anat Rec 1997;247:289–98.
9. Chevalier P, Tabib A, Meyronnet D, et al. Quantitative study of nerves of the human left atrium. Heart Rhythm 2005;2:518–22.
10. Marron K, Wharton J, Sheppard MN, et al. Distribution, morphology, and neurochemistry of endocardial and epicardial nerve terminal arborizations in the human heart. Circulation 1995;92:2343–51.
11. Singh S, Johnson PI, Javed A, Gray TS, Lonchyna VA, Wurster RD. Monoamine- and histamine-synthesizing enzymes and neurotransmitters within neurons of adult human cardiac ganglia. Circulation 1999;99:411–9.
12. Cao JM, Fishbein MC, Han JB, et al. Relationship between regional cardiac hyperinnervation and ventricular arrhythmia. Circulation 2000;101:1960–9.
13. Schafer MK, Schutz B, Weihe E, Eiden LE. Target-independent cholinergic differentiation in the rat sympathetic nervous system. Proc Natl Acad Sci U S A 1997;94:4149–54.
14. Arora R, Verheule S, Scott L, et al. Arrhythmogenic substrate of the pulmonary veins assessed by high-resolution optical mapping. Circulation 2003;107:1816–21.

15. Zhou S, Chang CM, Wu TJ, et al. Non-re-entrant focal activations in pulmonary veins in canine model of sustained atrial fibrillation. Am J Physiol Heart Circ Physiol 2002;283:H1244–52.
16. Hassink RJ, Aretz HT, Ruskin J, Keane D. Morphology of atrial myocardium in human pulmonary veins: a postmortem analysis in patients with and without atrial fibrillation. J Am Coll Cardiol 2003;42:1108–14.
17. Ho SY, Cabrera JA, Tran VH, Farre J, Anderson RH, Sanchez-Quintana D. Architecture of the pulmonary veins: relevance to radiofrequency ablation. Heart 2001;86:265–70.
18. Wit AL, Dillon SM, Coromilas J, Saltman AE, Waldacker B. Anisotropic re-entry in epicardial border zone in myocardial infarcts. Ann N Y Acad Sci 1990;591:86–108.
19. Hoover DB, Ganote CE, Ferguson SM, Blakely RD, Parsons RL. Localization of cholinergic innervation in guinea pig heart by immunohistochemistry for high-affinity choline transporters. Cardiovasc Res 2004;62:112–21.
20. Scherlag BJ, Nakagawa H, Jackman WM, et al. Electrical stimulation to identify neural elements on the heart: their role in atrial fibrillation. J Interv Card Electrophysiol 2005;13 Suppl 1:37–42.
21. Hsieh MH, Chiou CW, Wen ZC, et al. Alterations of heart rate variability after radiofrequency catheter ablation of focal atrial fibrillation originating from pulmonary veins. Circulation 1999;100:2237–43.
22. Aviado DM, Guevara AD. The Bezold-Jarisch reflex. A historical perspective of cardiopulmonary reflexes. Ann N Y Acad Sci 2001;940: 48–58.
23. Chiou CW, Eble JN, Zipes DP. Efferent vagal innervation of the canine atria and sinus and atrioventricular nodes—the third fat pad. Circulation 1997;95:2573–84.
24. Gray AL, Johnson TA, Ardell JL, Massari VJ. Parasympathetic control of the heart. II. A novel interganglionic intrinsic cardiac circuit mediates neural control of heart rate. J Appl Physiol 2004; 96:2273–8.